PHYSICS AND CHEMISTRY OF SOLID STATE
V. 26, No. 3 (2025) pp. 584-591
Section: Physics

DOI: 10.15330/pcss.26.3.584-591

Vasyl Stefanyk Carpathian National University

ФІЗИКА І ХІМІЯ ТВЕРДОГО ТІЛА
Т. 26, № 3 (2025) С. 584-591
Фізико-математичні науки

PACS: 66.35.+a; 74.25.fg

ISSN 1729-4428 (Print)
ISSN 2309-8589 (Online)

T. Potiatynnyk, O. Matkivskyi, V. Hovdiak, I. Horichok

Determination of the Fermi energy of electrons in lead telluride based on measurements of the Seebeck coefficient

Vasyl Stefanyk Carpathian National University, Ivano-Frankivsk, Ukraine, tetiana.potiatynnyk.22@pnu.edu.ua

The possibilities of using the model of dominance of one scattering mechanism of carriers for calculating the Fermi energy μ using experimental values of the Seebeck coefficient S_{exp} were analyzed. The specific electrical conductivity of n-PbTe:I was calculated in the relaxation time approximation with simultaneous consideration of many scattering mechanisms. The obtained Fermi energy values were compared with the values calculated as μ(S_{exp}). The influence of corrections to the Bloch form of wave functions and screening of scattering centers by carriers on the numerical values of mobilities and numerical values of Fermi energies determined in the model of dominance of one scattering mechanism was investigated.

Keywords: lead telluride, thermoelectric propertes, scattering mechanism, Fermi energy.

Received 24 Fbruary 2025; Accepted 10 September 2025.

Introduction

Analysis of the electronic subsystem of thermoelectric materials is an important aspect of the study of new and modification of the properties of known semiconductors [1-3]. One of the most urgent issues is the determination of the dominant carrier scattering mechanism and the calculation of the Fermi energy μ. The parameter μ can then be used to calculate almost all thermoelectric parameters of the material, in particular, the Seebeck coefficient *S*, the charge carrier concentration n, the carrier mobility *u*, the Lorentz number L_0.

If the carrier concentration n is known from Hall effect measurements, then μ can be easily calculated in the case of a parabolic semiconductor band with non-degenerate statistics:

$$n = N_C exp\left(\frac{\mu}{k_0 T}\right). \quad (1)$$

Here N_C is the density of states. The carrier concentration n itself is calculated from the experimentally measured Hall constant R_H:

$$n_H = \frac{A}{e_0 R_H}, \quad (2)$$

where *A* is the Hall factor. For non-degenerate materials with parabolic zones, the Hall factor is usually close to unity. But, as is known, the best thermoelectric materials are mainly characterized by non-parabolic zones and are weakly degenerate [1-3]. Then, for the correct calculation of the Hall factor, it is necessary to take into account the mechanisms of carrier scattering [4]. All this complicates the task of determining μ. In addition, the very setup of an experiment to study the Hall effect at high *T* is a relatively difficult task.

In view of the above, another approach to calculating μ is often used in the literature. Namely, determining μ from the experimental values of the Seebeck coefficient S [5-7]. Measuring S is a much simpler experiment than n_H, especially at high *T*, which, along with measuring the specific electrical conductivity, is always carried out to estimate the thermoelectric figure of merit. For a parabolic zone and non-degenerate statistics, *S* and μ are related by a simple dependence:

$$S = -\frac{k_0}{e_0}[r + 2 - \eta], \quad (3)$$

where $\eta = \mu / k_0 T$ is the reduced Fermi energy, r is the scattering parameter ($r = 0$ - scattering on the deformation potential of acoustic (DA) and optical (DO) phonons;

$r = 1$ - polarization scattering on the optical phonons (PO); $r = 2$ - scattering on ionized defects (ID)) [4].

With a known value of r, it will be technically easier to calculate μ from *S*. In addition, such a scheme does not require the value of the effective mass of carriers, as in the case of using formula (1), which is not known with sufficient accuracy for many new thermoelectric materials.

The problem remains the determination of the parameter *r*. For many materials, general trends in the implementation of certain mechanisms under different conditions are known. In particular, for A^4B^6 compounds, scattering is usually dominated by the deformation potential of acoustic phonons (DA). Under certain conditions, the influence of the deformation potential of optical phonons (DO) and the polarization potential of optical phonons (PO) may be significant. In particular, according to [8], at $n \geq 10^{19}$ cm^{-3} at room temperature, the contributions of PO, DO, DA are commensurate. Namely, such concentrations are characteristic of effective thermoelectric parameters.

Taking into account several mechanisms when calculating *S* is a relatively difficult task. Therefore, the calculation of μ is usually carried out in the DA dominance approximation [5-7], and the contribution of other mechanisms is neglected. In this work, we set the task of analyzing possible errors in estimating the electronic thermal conductivity and specific electrical conductivity with this approach. To do this, we calculated μ as a function of S_{exp} for the cases of dominance of each of the mechanisms (DA, DO, PO). We also calculated μ as a function of σ_{exp} for the same mechanisms and compared μ_S and μ_σ. In addition, μ was obtained by fitting σ to σ_{exp} while simultaneously taking into account all three mechanisms in the relaxation time approximation. The results of comparisons with each other were obtained in this way, which allowed us to draw conclusions about the accuracy of different approaches to determining the Fermi energy μ.

I. Calculation and results

The calculation of the Fermi energy based on the experimental values of the Seebeck coefficient was carried out by fitting the calculated value of S to the experimental S_{exp}, varying μ. In this case, the calculation of *S* was carried out according to the expression that takes into account the possibility of carrier degeneracy:

$$S = -\frac{k_0}{e_0}\left[\frac{I^1_{r+1,2}(\eta,\beta)}{I^0_{r+1,2}(\eta,\beta)} - \eta\right]. \quad (4)$$

Here $I^{\mathrm{m}}_{\mathrm{n,k}}(\eta,\beta)$ is the Fermi integral:

$$I^{\mathrm{m}}_{\mathrm{n,k}}(\eta,\beta) = \int_0^\infty \left(-\frac{\partial f_0}{\partial x}\right)\frac{x^m(x+\beta x^2)^n dx}{(1+2\beta x)^k}, \quad (5)$$

Where $x = \frac{E}{k_0T}$ is the reduced energy, $\eta = \frac{\mu}{k_0T}$. is the reduced Fermi energy, $\beta = \frac{k_0T}{E_g}$ is the nonparabolicity index, $f_0 = \frac{1}{1+e^{x-\eta}}$ is the Fermi function.

The μ_S values obtained in the described way were used to calculate the specific electrical conductivity:

$$\sigma = une, \quad (6)$$

where *u* is the carrier mobility.

The carrier concentration was defined as:

$$n = \frac{(2m_{d,0}kT)^{\frac{3}{2}}}{3\pi^2\hbar^3} I^0_{3/2,0}(\eta,\beta), \quad (7)$$

where $m_{d,0}$ is the effective mass of the density of states at the bottom of the zone, and the mobility [4]:

$$u = e\frac{\tau_0(T)}{m_{n,0}} \cdot \frac{I^0_{r+1,2}(\eta,\beta)}{I^0_{3/2,0}(\eta,\beta)}. \quad (8)$$

Here $m_{n,0}$ is the effective mass at the bottom of the zone, τ_0 is the relaxation time of carriers. In the case of scattering on the deformation potential of acoustic phonons:

$$\tau_{0r}(T) = \frac{2\pi\hbar^4\rho v_0^2}{(2m_{n,0}k_0T)^{\frac{3}{2}}E_1^2} \quad (9)$$

where ρ = 8.24 g/cm^3 [8], E_1:=15 eV [8], v_0 = 1.92 km/s [9]), r = 0.

When scattering on the deformation potential of optical phonons (for $k_0T >> \hbar\omega_0$):

$$\tau_{0r}(T) = \frac{2}{\pi}\left(\frac{\hbar\omega_0}{E_0}\right)^2 \frac{\hbar^2a^2\rho}{(2m_{n,0}k_0T)^{\frac{3}{2}}}, \quad (10)$$

where $\hbar\omega_0 = k\,\theta$ (θ = 157,8 K [10, 11]), a = 6.461 Å [8], E_0:=26 eV [8], , r = 0.

When scattering on the polarization potential of optical phonons (for $k_0T >> \hbar\omega_0$):

$$\tau_{0r}(T) = \frac{\hbar^2}{e^2\sqrt{2m_nk_0T}\left(\frac{1}{\chi_\infty}-\frac{1}{\chi_0}\right)}, \quad (11)$$

where χ_∞ = 32,6 [8]; χ_0 = 400 [8]; r = 1.

When calculating for all scattering mechanisms, corrections for the Bloch form of wave functions were taken into account (in the two-band approximation), and for polar optical phonons, an additional correction for the screening of scattering centers by free charge carriers.

According to [4], this correction for acoustic phonons is defined as:

$$F_{ak}(k) = 1 - \frac{10}{3}L + \left[\frac{191}{60} + \frac{11}{60}\left(\frac{v_L}{v_T}\right)^2\right]L^2, \quad (12)$$

where v_L and v_T are the longitudinal and transverse components of the speed of sound. When scattering on the deformation potential of optical phonons [4]:

$$F_{KP} = 1 - \frac{8}{3}L + \frac{13}{6}L^2 \quad (13)$$

And when scattering on the polarization potential of optical phonons [4]:

$$F'_{PO} = 1 - \frac{2}{\xi}\ln(1+\xi) + \frac{1}{1+\xi} - \frac{1}{2}(4L - L^2)B + L^2C \quad (14)$$

$\xi = (2kr_0)^2$, where k is the wave number, r_0 is the shielding radius.

In the above formulas:

$$L = \frac{E}{E_g+2E}, \quad B = 1 - \frac{4}{\xi} - \frac{2}{\xi(1+\xi)} + \frac{6}{\xi^2}\ln(1+\xi), \quad C = 1 - \frac{3}{\xi} + \frac{9}{\xi^2} + \frac{3}{\xi^2(1+\xi)} - \frac{12}{\xi^3}\ln(1+\xi)$$

The shielding radius in the calculation of ξ was determined as [4] $r_0^2 = \frac{\chi_0 k_0 T}{6\pi e_0^2 n} \cdot \frac{I^0_{3/2,0}(\eta,\beta)}{I^0_{1/2,-1}(\eta,\beta)}$, and the wave number $k = \sqrt{\frac{2m_{n,0}}{\hbar^2}\bar{E}\left(1+\frac{\bar{E}}{E_g}\right)}$. The value of the energy included in this expression was determined by averaging, according to [4]: $\bar{E} = \frac{1}{n}\int_0^\infty E \cdot g(E) \cdot f_0(E,\mu)dE$, and $n = \int_0^\infty g(E) \cdot f_0(E,\mu)dE$. The density of states [4]:

$$g(E) = \frac{(2m_{d,0})^{\frac{3}{2}}}{2\pi^2\hbar^3} E^{\frac{1}{2}}\left(1+\frac{E}{E_g}\right)^{\frac{1}{2}}\left(1+\frac{2E}{E_g}\right).$$

The correction was taken into account by dividing the corresponding values of τ_0 by the correction.

For the analysis, the $S(T)$ and $\sigma(T)$ data for iodine-doped lead telluride PbTe:I as one of the best thermoelectric materials were used. The impurity I does not create localized energy levels and is one of the most effective donors in PbTe. For this material, there is a lot of experimental data in the literature, which makes it a good model object. We used the $S(T)$, $\sigma(T)$ data from [12].

Fig. 1 presents the results of calculating the Fermi energy and other thermoelectric parameters in the scattering dominance approximation on the deformation potential of acoustic phonons. Fig. 1.a shows the temperature dependence of the Fermi energy μ_S obtained from the experimental dependence $S(T)$ (points in Fig. 1, c) using formula 4. Using the μ_S obtained in this way, the specific electrical conductivity was calculated using formula (6) (Fig. 1, d). We see that the difference between the calculated $\sigma(T)$ and the experimental values is ≈ 1000 S/cm and is practically constant over the entire temperature range. At 550 K, the relative error will be ≈ 50%, and at 300 K – ≈ 20%.

If the Fermi level is determined not from $S_{exp}(T)$, but from $\sigma_{exp}(T)$, then the obtained values of μ_σ will differ significantly from μ_S (Fig. 1, a). The procedure was implemented by fitting the conductivity calculated by formula (6) to the experimental values by varying μ. When μ_σ is further used to calculate $S(T)$, we see that the difference from the experimental values is ≈ 30%. Also, using μ_S and μ_σ, the calculation of L_0 was carried out (Fig. 1, b). Unlike σ and S, the differences here turned out to be somewhat smaller. In the entire temperature range, they did not exceed 10%. The obtained results make it possible to estimate possible errors when using this approach.

When using the DO and PO dominance model, the differences between μ_S and μ_σ become even greater (Fig. 2, 3). Accordingly, for the calculated and experimental dependences $S(T)$ and $\sigma(T)$, the differences are also more significant. Therefore, DA can indeed be considered decisive for this material. However, since the

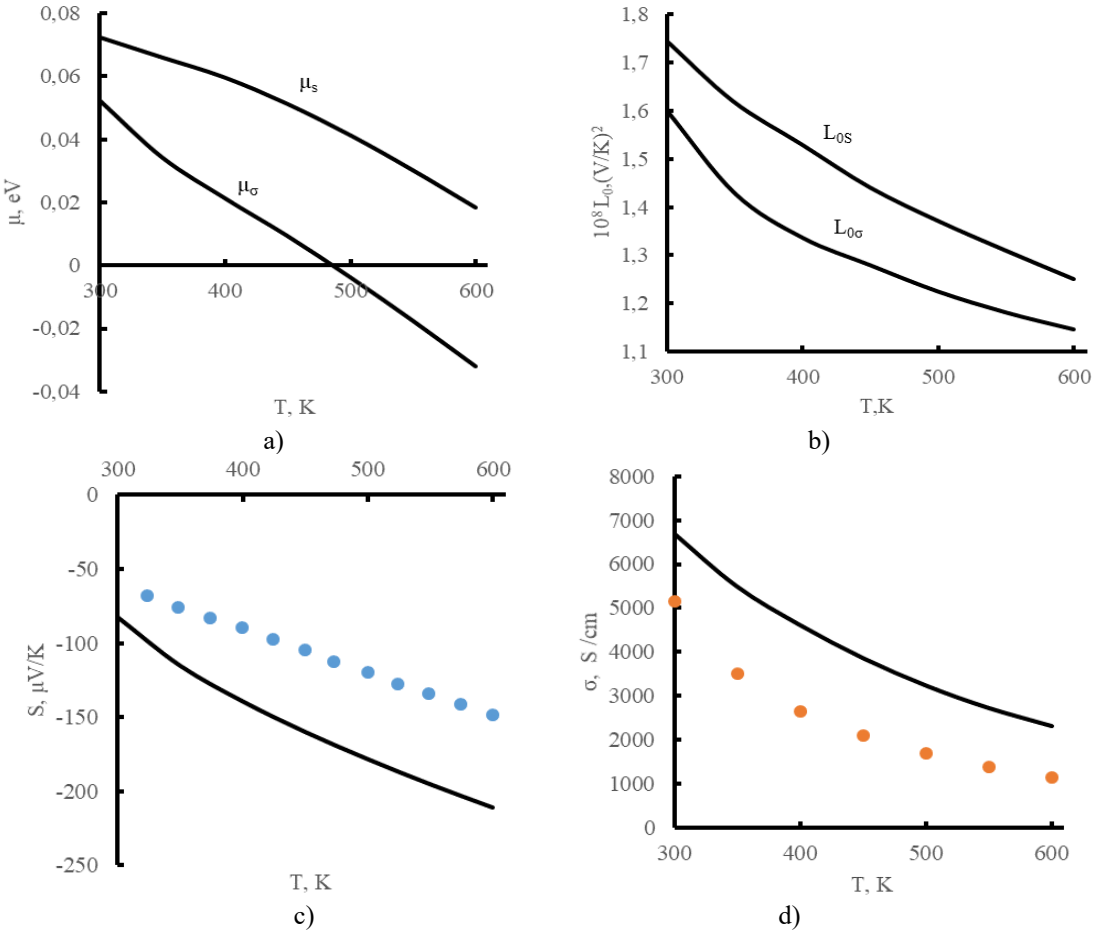

Fig. 1. a) – temperature dependences of the Fermi energy of electrons obtained using the assumption of DA dominance (μ_S calculated from the experimental dependence $S(T)$, and μ_σ calculated from the experimental dependence $\sigma(T)$); b) – calculated values of the Lorentz constant for two values of the Fermi energy presented in Figure a; c) experimental dependence $S(T)$ (dots) and calculated using the values of μ_σ; d) – experimental dependence $\sigma(T)$ (dots) and calculated using the values of μ_S. Experimental data – [11].

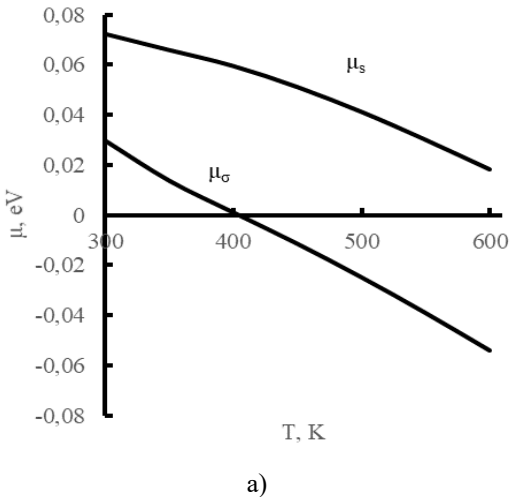

a)

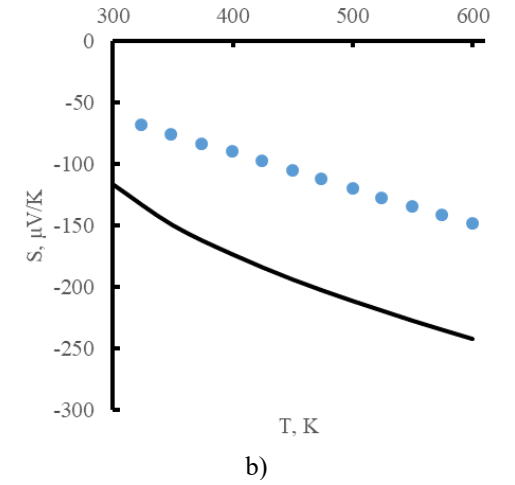

b)

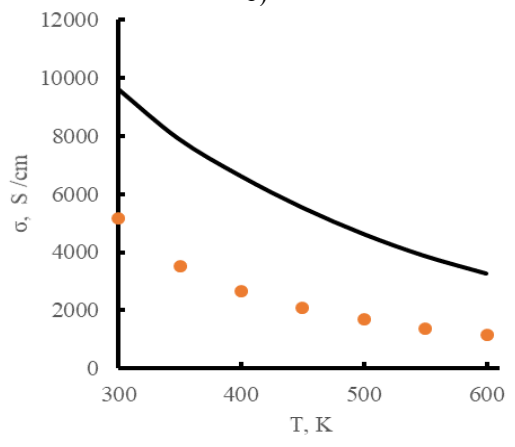

c)

Fig. 2. a) – temperature dependences of the Fermi energy of electrons obtained using the assumption of DO dominance (μ_S calculated from the experimental dependence $S(T)$, and μ_σ calculated from the experimental dependence $\sigma(T)$); b) – experimental dependence $S(T)$ (dots) and calculated using the values of μ_σ; c) – experimental dependence $\sigma(T)$ (dots) and calculated using the values of μ_S.
Experimental data – [11].

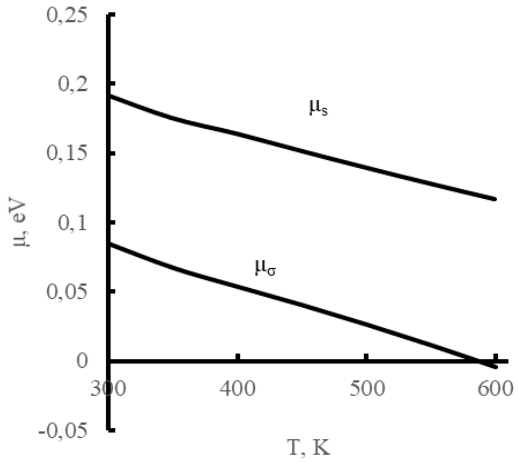

a)

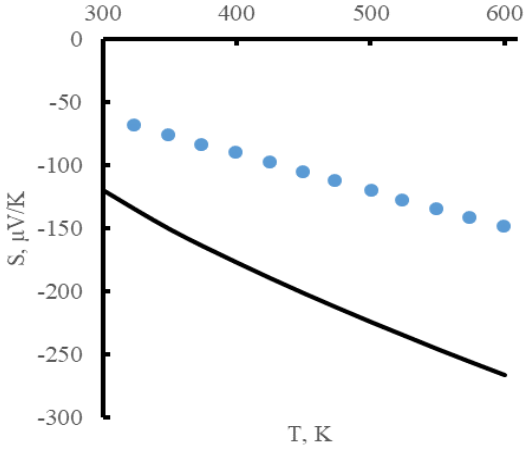

b)

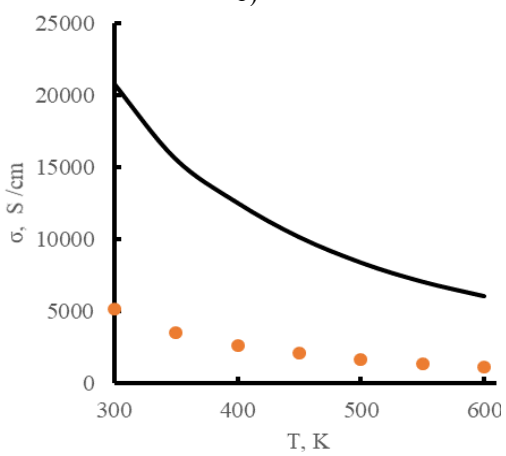

c)

Fig. 3. a) – temperature dependences of the Fermi energy of electrons obtained using the assumption of PO dominance (μ_S calculated from the experimental dependence $S(T)$, and μ_σ calculated from the experimental dependence $\sigma(T)$); b) – experimental dependence $S(T)$ (dots) and calculated using the values of μ_σ; c) – experimental dependence $\sigma(T)$ (dots) and calculated using the values of μ_S.
Experimental data – [11].

results do not coincide when $S(T)$ and $\sigma(T)$ are "cross-calculated", the contribution of other mechanisms is obviously quite significant.

To assess how much the result of the Fermi energy calculation can change when taking into account DA, DO, PO simultaneously, the calculation of $\sigma(T)$ was carried out. At the same time, by varying μ, the best possible agreement of the calculated dependence $\sigma(T)$ with the experimental one was achieved. In this case, the mobility included in (6) was calculated using the Mathissen rule:

$$\frac{1}{u} = \frac{1}{u_{DA}} + \frac{1}{u_{DO}} + \frac{1}{u_{PO}} \qquad (15)$$

Fig. 4. presents the results of the calculation of the mobility for impurity-free PbTe and a comparison of its results with the experimental data of work [8]. We see that in the region $n \geq 10^{19}$ cm^{-3} our calculated values of u agree very well with the experimental ones.

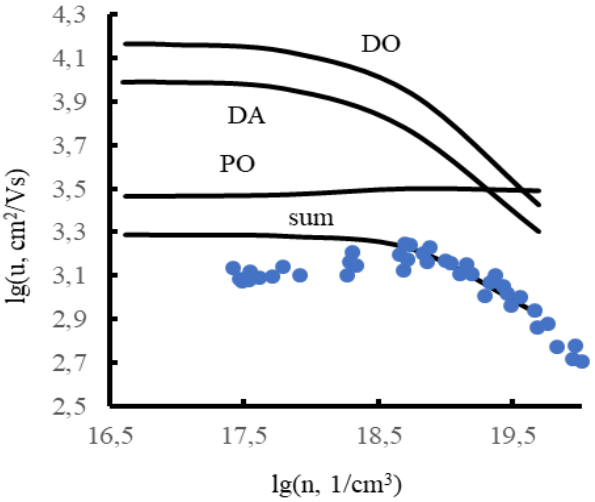

Fig. 4. Dependence of electron mobility in PbTe on their concentration at 300 K. Sum – mobility obtained taking into account three scattering mechanisms (DA+DO+PO); DA – partial contribution due to scattering on the deformation potential of acoustic phonons; DO – partial contribution due to scattering on the deformation potential of optical phonons; PO – partial contribution due to scattering on the polarization potential of optical phonons. Points – experimental data [8].

Fig. 5a shows the temperature dependence of the electron mobility obtained when fitting to $\sigma_{exp}(T)$ with partial contributions from each of the mechanisms. And Fig. 5b shows the results of a similar calculation, but without taking into account corrections for non-parabolicity (in calculating the Fermi integral), as well as without corrections for the Bloch form of the wave functions and screening (in calculating the relaxation time). We see that taking into account all mechanisms simultaneously, the contribution of DA and PO turns out to be approximately commensurate for both calculation options. However, in the case of taking into account all corrections, the numerical values of u agree much better with the experimental ones, while without taking them into account the difference is quite significant.

If we analyze the experimental dependence of $\sigma(T)$ in logarithmic coordinates, the slope of the obtained straight line is -2.1 (fig. 6). According to [4], for electrons

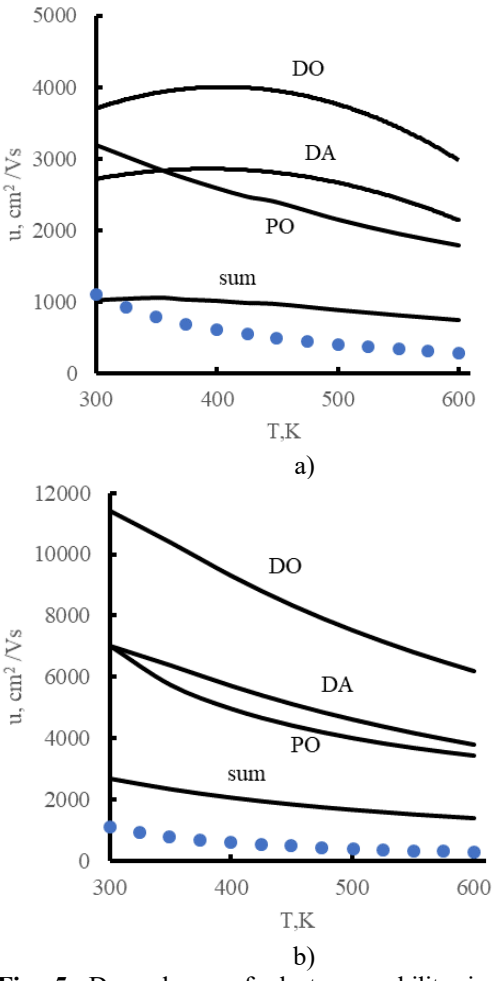

Fig. 5. Dependence of electron mobility in PbTe:I on temperature. Sum – mobility obtained taking into account three scattering mechanisms (DA+DO+PO); DA – partial contribution due to scattering on the deformation potential of acoustic phonons; DO – partial contribution due to scattering on the deformation potential of optical phonons; PO – partial contribution due to scattering on the polarization potential of optical phonons. Points – experimental data [12].

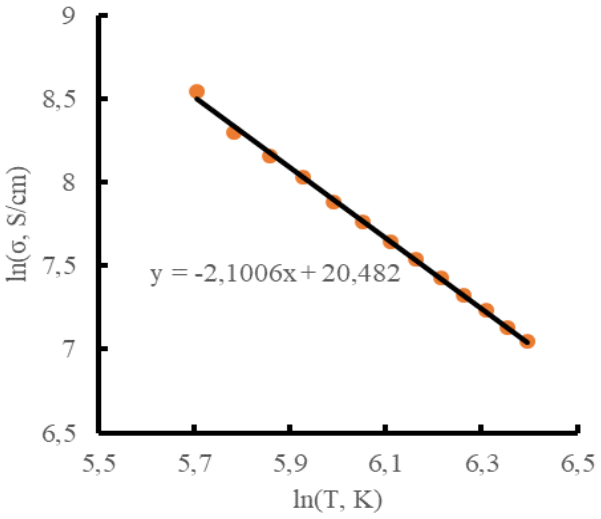

Fig. 6. Linear approximation of the dependence of the specific electrical conductivity on temperature in logarithmic coordinates for PbTe:I crystals. Points are experimental data [12], straight line is the approximation dependence.

scattering on the deformation potential of acoustic phonons (DA) this value should be -2.5, and for scattering on the polarization potential of optical phonons (PO) – -1.1. Thus, in the studied material, one should really expect the simultaneous action of several scattering mechanisms.

It is important that, in addition to the good agreement of the calculated dependence u(T) with the experimental one, only for the model that takes into account three scattering mechanisms simultaneously it is possible to obtain the calculated carrier concentration $n = 3.1\ 10^{19}$ cm^{-3}, which corresponds to the experimental value at 300 K $n_{exp} = 2.9\ 10^{19}$ cm^{-3}. If, for example, the DA dominance model was considered, then the carrier concentration calculated from the μ_S and μ_σ values is $n_\sigma = 0.5\ 10^{19}$ cm^{-3}, $n_S = 0.8\ 10^{19}$ cm^{-3}, which is many times less than the experimental value.

It is worth paying attention to the influence of the above-described corrections on the numerical values of the Fermi energy and other material parameters calculated on its basis. Let us recall that all the above results, except for Fig. 5.b, were obtained taking them into account. When taking into account only some of them, it is also possible to obtain results that are in good agreement with the experimental ones. For example, if we do not take into account the non-parabolicity of the PbTe conduction band, then for the DA dominance model the obtained μ_S(T) values practically coincide with the calculation results when taking into account all three mechanisms simultaneously (Fig. 7). According to such a result, it could be said that DA is indeed the only dominant

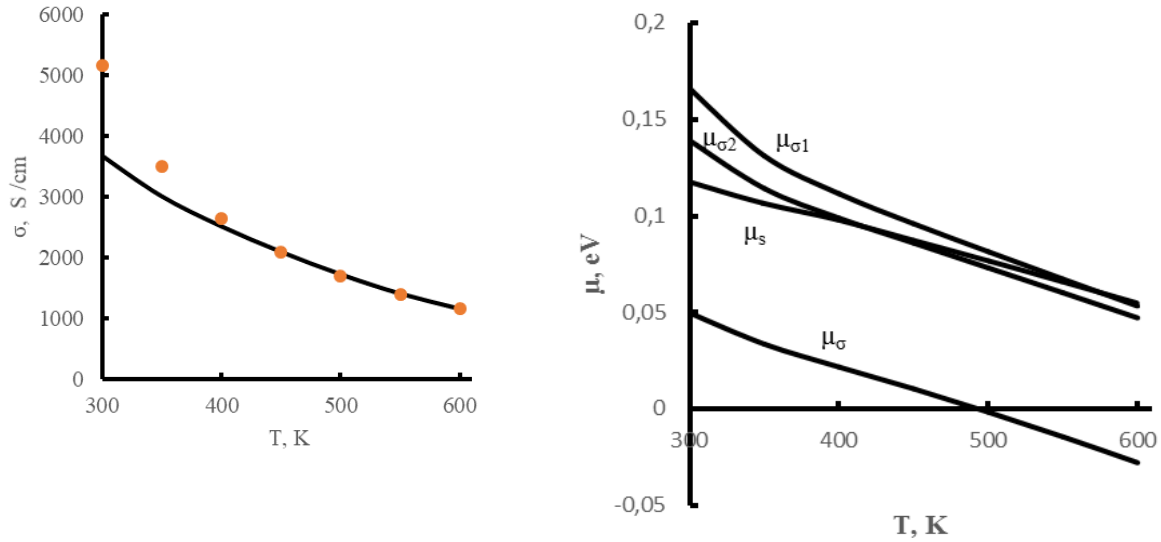

a) b)

Fig. 7. Temperature dependences of the Fermi energy of electrons μ calculated from the experimental dependence $S(T)$ and $\sigma(T)$, using different approximations: μ_S – calculated from the experimental dependence $S(T)$, and μ_σ – from the experimental dependence $\sigma(T)$, using the assumption of DA dominance; $\mu_{\sigma 1}$ - calculation in the relaxation time approximation with simultaneous consideration of three carrier scattering mechanisms (DA+DO+PO); $\mu_{\sigma 2}$ - similar to $\mu_{\sigma 1}$, but the non-parabolicity of the zones, corrections for screening for PO, and the Bloch divergence of wave functions are not taken into account.

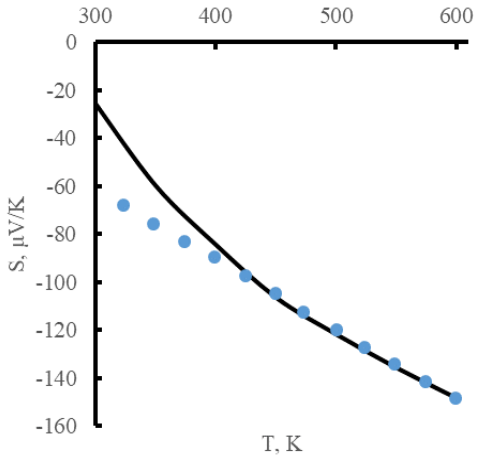

a) b)

Fig. 8. a) experimental dependence S(T) (points [11]) and calculated using the values of μ_σ; c) experimental dependence $\sigma(T)$ (points [11]) and calculated using the values of μ_S. The calculations were carried out in the DA dominance approximation taking into account the nonparabolicity of the zones but without taking into account the correction for the Bloch form of the wave function.

scattering mechanism. However, if we calculate the specific electrical conductivity based on such $\mu_S(T)$ values, the obtained values will differ even more from the experimental ones than in Fig. 1.d.

Another interesting result is obtained for the DA dominance model, if we take into account the non-parabolicity of the conduction band, but do not take into account the corrections for the Bloch form of the wave functions. If for such a model we obtain $\mu_S(T)$ from the S(T) dependence and then use it to calculate S(T), then for temperatures above 350 K we obtain almost perfect agreement with the experiment. A similar result can be obtained if we calculate $\mu_\sigma(T)$ from the experimental dependence $\sigma_{exp}(T)$ and calculate S(T) on its basis. This result can also be accepted as confirmation of the dominance of one DA mechanism (Fig. 8). However, the carrier concentration at T = 300 K is 0.8 10^{19} cm^{-3}, which is more than three times different from the experimental value.

Such results can most likely be argued in each specific case. However, in the general case, such simplified schemes do not seem justified. And quantitatively, the calculation results are in the best agreement with the experimental ones for the model that takes into account several scattering mechanisms and all the corrections described above.

Conclusions

The choice of the dominant scattering mechanism model significantly affects the calculated values of the Fermi energy μ_S based on the experimental values of $S(T)$. The obtained numerical values for the single scattering mechanism dominance model vary from $\approx E_C + 0.025$ eV for DO to $\approx E_C + 0.2$ eV for PO at 300 K.

According to the results of the calculations, the numerical values of μ obtained within the framework of the scattering dominance model on the deformation potential of acoustic phonons, when further used to calculate the main thermoelectric parameters (Seebeck coefficient, specific electrical conductivity, and Lorentz number), lead to results that differ from the experimental ones by 10-50%.

Taking into account three scattering mechanisms simultaneously allows achieving significantly better agreement between the calculated and experimental material parameters. Moreover, according to the obtained results, for the studied material PbTe:I, the partial contributions of the DA and PO mechanisms in the temperature range 300-600 K are practically the same.

When calculating the kinetic properties of PbTe, it is important to take into account the degeneracy of carriers, non-parabolicity of the band, and corrections for screening and the Bloch form of the wave functions. Otherwise, the numerical values of the calculated and experimental parameters may differ by half.

Potiatynnyk T. – student;
Matkivskyi O. – Candidate of Physical and Mathematical Sciences, Senior Researcher;
Hovdiak V. – postgraduate;
Horichok I. – Doctor of Physical and Mathematical Sciences, Professor.

[1] Z.M. Gibbs, F. Ricci, G. Li, H. Zhu, K. Persson, G. Ceder, G. Hautier, A. Jain, G. J. Snyder, *Effective Mass and Fermi Surface Complexity Factor from Ab Initio Band Structure Calculations*. Comput. Mater, 3 (1), 1 (2017); https://doi.org/10.1038/s41524-017-0013-3.
[2] Y. Pei, X. Shi, A. LaLonde, H. Wang, L. Chen, G. J. Snyder, *Convergence of Electronic Bands for High Performance Bulk Thermoelectrics.* Nature, 473 (7345), 66 (2011); https://doi.org/10.1038/nature09996.
[3] O.M. Matkivskyi, V.R. Balan, M.O. Halushchak, I.B. Dadiak, G.D. Mateik, I.V. Horichok, *Thermal conductivity of GeBiTe solid solutions.* Physics And Chemistry Of Solid State, 25 (1), 189 (2024); https://doi.org/10.15330/pcss.25.1.185-190.
[4] B.M. Askerov, Electron Transport Phenomena in Semiconductors. 1994. https://doi.org/10.1142/1926.
[5] Y. Xiao, W. Li, C. Chang, Y. Chen, L. Huang, J. He, L.-D. Zhao, *Synergistically optimizing thermoelectric transport properties of n-type PbTe via Se and Sn co-alloying.* Journal of Alloys and Compounds. (2017); https://doi.org/10.1016/j.jallcom.2017.06.296.
[6] T. Parashchuk, Z. Dashevsky, K. Wojciechowski, *Feasibility of a High Stable PbTe:In Semiconductor for Thermoelectric Energy Applications.* J. Appl. Phys., 125 (24), 245103 (2019); https://doi.org/10.1063/1.5106422.
[7] Z. Dashevsky, I. Horichok, M. Maksymuk, A.R. Muchtar, B. Srinivasan, T. Mori, *Feasibility of high performance in p-type Ge1-xBixTe materials for thermoelectric modules.* J Am Ceram Soc., 1 (2022); https://doi.org/10.1111/jace.18371.
[8] D.M. Zayachuk, *The Dominant Mechanisms of Charge-Carrier Scattering in Lead Telluride*. Semiconductors, 31 (2), 173 (1997); https://doi.org/10.1134/1.1187322.
[9] R. Knura, T. Parashchuk, A. Yoshiasa, K.T. Wojciechowski, *Origins of Low Lattice Thermal Conductivity of $Pb_{1-x}Sn_xTe$ Alloys for Thermoelectric Applications.* Dalt. Trans., 50 (12), 4323 (2021); https://doi.org/10.1039/d0dt04206d.
[10] O. Khshanovska, T. Parashchuk, I. Horichok, *Estimating the upper limit of the thermoelectric figure of merit in n- and p-type PbTe.* Materials Science in Semiconductor Processing, 160, 107428 (2023); https://doi.org/10.1016/j.mssp.2023.107428.
[11] D. M.Freik, S. I.Mudryi, I. V.Gorichok, R. O.Dzumedzey, O. S.Krynytskyi, & T. S. Lyuba, (2014). Charge carrier scattering mechanisms in thermoelectric PbTe: Sb. *Ukrainian journal of physics*, (59,№ 7), 706-711; https://doi.org/10.15407/ujpe59.07.0706.

[12] P. Yanzhong, A.D. LaLonde, H. Wang, nd G.J. Snyder, *Low effective mass leading to high thermoelectric performance*. Energy Environ. Sci., 5, 7963 (2012); https://doi.org/10.1039/c2ee21536e.

Т. Потятинник, О. Матківський, В. Говдяк, І. Горічок

Визначення енергії Фермі електронів у телуриді свинцю на основі вимірювань коефіцієнта Зеебека

Карпатський національний університет імені Василя Стефаникам. Івано-Франківськ, Україна

Проаналізовано можливості використання моделі домінування одного механізму розсіювання носіїв для розрахунку енергії Фермі μ використовуючи експериментальні значення коефіцієнта Зеебека Sexp. Проведено розрахунок питомої електропровідності n-PbTe:I в наближенні часу релаксації з одночасним врахуванням багатьох механізмів розсіювання. Отримані при цьому значення енергії Фермі співставлено з величинами розрахованими як μ(Sexp). Досліджено вплив поправок на блохівський вигляд хвильових функцій та екранування носіями розсіюючих центрів на числові значення рухливостей і визначених в моделі домінування одного механізму розсіювання числових значень енергій Фермі.

Ключові слова: телурид свинцю, термоелектричні властивості, механізми розсіювання, енергія Фермі.